

Passive Microwave Remote Sensing of Snow Constrained by Hydrological Simulations

Chi-Te Chen, *Student Member, IEEE*, Bart Nijssen, Jianjun Guo, Leung Tsang, *Fellow, IEEE*, Andrew W. Wood, Jenq-Neng Hwang, *Fellow, IEEE*, and Dennis P. Lettenmaier

Abstract—This paper describes a snow parameter retrieval algorithm from passive microwave remote sensing measurements. The three components of the retrieval algorithm include a dense media radiative transfer (DMRT) model, which is based on the quasicrystalline approximation (QCA) with the sticky particle assumption, a physically-based snow hydrology model (SHM) that incorporates meteorological and topographical data, and a neural network (NN) for computational efficient inversions. The DMRT model relates physical snow parameters to brightness temperatures. The SHM simulates the mass and heat balance and provides initial guesses for the neural network. The NN is used to speed up the inversion of parameters. The retrieval algorithm can provide speedy parameter retrievals for desired temporal and spatial resolutions. Four channels of brightness temperature measurements: 19V, 19H, 37V, and 37H are used. The algorithm was applied to stations in the northern hemisphere. Two sets of results are shown. For these cases, we use ground-truth precipitation data, and estimates of snow water equivalent (SWE) from SHM give good results. For the second set, a weather forecast model is used to provide precipitation inputs for SHM. Additional constraints in grain size and density are used. We show that inversion results compare favorably with ground truth observations.

Index Terms—Dense media, random media, remote sensing, snow.

I. INTRODUCTION

ESTIMATES of snow parameters such as snow depth or snow water equivalent (SWE) are important for many geoscience problems. For example, long-term monitoring of snow storage is critical for assessing global climate changes and estimating techniques of SWE are common inputs to water resource management and flood forecasting. Algorithms for snow parameter retrieval have been developed for many years [1]–[12]. Even though the snowpack telemetry (SNOTEL) network provides daily observations of SWE at ground stations, the network of surface observations results in a very sparse set of point measurements over the areas. Furthermore, for remote areas, such as mountainous regions that contain significant amount of snow, snowpack surface observations are usually not available. For such areas, passive microwave remote sensing data, e.g., scanning multichannel microwave radiometer (SMMR) and special sensor microwave imager (SSM/I) measurements, offers a more comprehensive means of measuring snowpacks.

Manuscript received April 11, 2000; revised January 21, 2001.

C.-T. Chen, J. Guo, L. Tsang, and J.-N. Hwang are with the Department of Electrical Engineering, University of Washington, Seattle, WA 98195-2500 USA.

B. Nijssen, A. Wood, and D. P. Lettenmaier are with the Department of Civil Engineering, University of Washington, Seattle, WA 98195-2700 USA.

Publisher Item Identifier S 0196-2892(01)05480-8.

To make use of passive microwave remote sensing data, linear regression techniques have been studied for years [1]–[7], [9], [12]. In linear regression algorithms, a subset of brightness temperature measurements is used to infer snow depth. In some models, empirical relations for linear regression techniques are formulated by theoretical scattering models and radiative transfer theory [2], [5], [9]. Mie [1], [7] and Rayleigh [13], [14] scattering of single size particles with independent scattering assumption were also used. In some models, the coefficients for regression algorithms are determined empirically by linearly fitting differences of brightness temperatures of horizontal polarization at 19 and 37 GHz [12]. For example, in the Goddard Space Flight Center (GSFC) algorithm [9], different coefficients are derived for different regions of the world. The regression coefficients of each region are determined by choosing a fixed grain size, 0.4 mm for interior areas of Eurasia and 0.3 mm elsewhere in Eurasia and North America, and finding a linear fit of differences in brightness temperatures.

Besides snow depth, snow parameters such as grain size and density affect passive microwave remote sensing measurements. To simplify the retrieval problem, most investigators use single density and single grain size to develop their models. Based on Mie and Rayleigh scattering models [1], [14], however, brightness temperatures have strong dependence on the grain size. Results of snow depth retrievals can be completely different depending on the choice of grain size.

In the passive remote sensing of snow, brightness temperatures of both vertical and horizontal polarizations at 19 and 37 GHz (19V, 19H, 37V, and 37H) are measured. Unlike some algorithms, in which only a subset of brightness temperature measurements is used, absolute values of four channels of brightness temperatures are utilized in our algorithm as they all contain information. In our approach, we use *a priori* estimates of snow parameters given by a physically based snow hydrology model (a snow accumulation and ablation model) which incorporates meteorological and topographical information. A dense media radiative transfer (DMRT) model is used to relate the snow physical parameters to the emission and scattering of the media, and a neural network is used for speedy retrieval and systematically quantifying the constraints. This algorithm is an extension of the algorithm by Wilson *et al.* [10]. Several improvements are made. First, this DMRT model is based on the quasicrystalline approximation (QCA) with a sticky particle model. In the sticky particle assumption, particles are allowed to adhere together to form clusters. At low frequencies, they scatter as particles with larger effective sizes while at high frequencies, the clustering effect disappears and they exhibit the usual dense media scat-

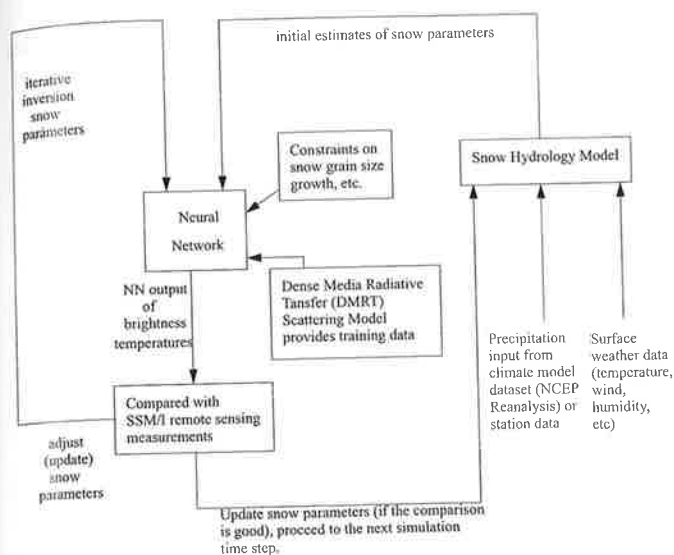


Fig. 1. Flow chart for the snow parameter retrieval algorithm. The precipitation input for the snow hydrology model is either from ground weather stations or from the NCEP reanalysis project. The neural network performs either nonconstrained or constrained inversions.

tering properties. Roughness and atmospheric effects are taken into account in the parameter retrieval algorithm. Second, for real-time applications, weather forecast models are used to provide precipitation inputs for the snow hydrology model. In practical implementations, real time precipitation data may not be available. Furthermore, precipitation stations are also sparsely distributed. Thus it is important to test the applicability of the algorithm using weather forecast model as precipitation input. In this paper, we use the National Center for Environmental Prediction (NCEP), weather forecast model as the source for precipitation inputs. Third, during the inversion scheme, constraints on snow grain size growth and fractional volume are imposed.

Section II describes the methodology of the algorithm. Section III provides the details of each individual components of the algorithm. In Section IV, we compare results based on the parameter retrieval algorithm with ground observations for stations in the Northern Hemisphere.

II. METHODOLOGY

The procedures of the parameter retrievals are given in the flow chart of Fig. 1. Each step is listed below while more detailed discussions of each component are provided in the next section.

The procedure can be divided into two stages: neural network training and inversion. The synaptic weights of the neurons are determined during the training stage. The training data consists of combinations of snow parameters and the corresponding brightness temperatures calculated by the DMRT model. The value ranges of snow parameters are chosen according to observations of snow terrain. During the neural network training, snow parameters are used as input and brightness temperatures as output. After the training is completed, the weights in the neural network are determined. We can then proceed to the parameter inversion stage. Note that further constraints can be applied during the inversion. It requires some preprocessing to es-

tablish the model of constraints. The following steps describe the inversion algorithm.

- 1) A snow hydrology model driven by topographical and meteorological data is used to provide initial estimates for the neural network. Topographical characteristics are determined from digital elevation model (DEM) data. Meteorological inputs include surface weather data, such as temperature, wind speed, humidity, and precipitation, either from ground station measurements or the weather forecast model. The output from the snow hydrology model consists of snow depth, density (fractional volume), snow grain size and snow temperature, which are then used as input to the neural network.
- 2) Brightness temperatures are first computed by the neural network for snow parameters given by the snow hydrology model.
- 3) Output brightness temperatures are then compared with satellite SSM/I brightness temperature measurements. The differences are used to adjust (update) snow parameters, which are then used as new input to neural network.
- 4) We then compute brightness temperatures through the neural network with the adjusted snow parameters and repeat Step 3). This iterative approach is repeated until output brightness temperatures from the neural network converge upon SSM/I brightness temperature measurements.
- 5) When the snow parameters converge, i.e., calculated brightness temperatures agree with observed ones, the snow parameters are then used as the updated input to the snow hydrology model, and the snow model proceeds to the next time step.

The updating procedure is only performed when all of the following conditions are met simultaneously: 1) the snow parameters are in the range of the training dataset, for example, the snow depth has to be between 0 cm and 100 cm; 2) observed brightness temperatures fall into the range of calculated brightness temperatures in the training data; and 3) no liquid water is in the snowpack, i.e., the snowpack is dry. Note that microwaves at 19 and 37 GHz cannot penetrate wet snowpacks. The liquid water content is modeled by the snow hydrology model and the snowpack is considered wet when liquid water content is over a certain threshold. When the snowpack is wet, which usually happens at the end of snow seasons when air temperature is above 0 °C, no updating is performed and the snow parameters are the ones given by the snow hydrology model. To simplify the problem, all sites in this paper are modeled without vegetation cover.

III. IMPLEMENTATION OF METHODOLOGY

We describe the three major components in our algorithm in this section.

A. Dense Media Radiative Transfer Model

The DMRT theory describes scattering, absorption and emission of a dense medium. It relates physical parameters, such as density, particle sizes and layer thickness to brightness temperatures. Previously, a DMRT model derived from the qua-

sicrystalline approximation with coherent potential (QCA-CP) and correlated ladder approximation was developed [15]. The Rayleigh phase function was obtained in the derivation. QCA-CP is a nonlinear approximation and the solution is limited to small particles. For frequencies of 19 and 37 GHz, a DMRT model valid up to moderate size particles is desired. To achieve this, a DMRT model based on the QCA was developed recently [16]. Higher order multipoles in addition to dipoles terms are taken into account.

Because grain sizes are much smaller than wavelength, scattering model usually exhibits frequency to the fourth power dependence. The sticky particle model is also introduced in the recent DMRT model [16]. In the sticky particle model, the snow grains are allowed to stick together to form clusters. At low frequencies, particles scatter as a particle with larger effective size, thus, the scattering is larger than that of independent scattering. At high frequencies, the clustering effect disappears and particles scatter like usual dense media and the scattering is less than that of independent scattering. The frequency dependence of the sticky particle model is thus weaker than frequency to the fourth power and can better match the observed frequency dependence.

In the DMRT model [16], the QCA with the sticky particle assumption is used to calculate the effective propagation constant and coherent transmission into dense media from physical snow parameters such as particle sizes and fractional volumes. The distorted Born approximation is used to calculate the phase matrix of DMRT, which is bistatic scattering coefficient per unit volume in a differential volume.

For passive microwave remote sensing applications, other effects, such as roughness and atmospheric effects, also have to be taken into account.

We use the empirical Q - H model for the rough interface between snow and ground [17]

$$R_{\alpha}(\theta) = [(1 - Q)r_{\alpha}(\theta) + Qr_{\beta}(\theta)]e^{-H \cos^2 \theta} \quad (1)$$

where

- α, β = v, h ;
- Q and H empirical constants;
- r_{α} and r_{β} Fresnel reflectivities;
- R_{α} modified reflectivity;
- Q mixing factor between two polarizations.

For smaller values of Q , the contrast between two polarizations is larger. Thus, the value of Q can be determined by differences between vertical and horizontal polarized measurements. The parameter H affects absolute measurements of brightness temperatures. For thin snowpack, reflectivities at the interfaces instead of volume scattering of the media dominate brightness temperatures. Thus, H value can be determined from brightness temperature measurements when the snowpack is thin. In this study, the mixing factor Q is chosen as 0.4 and $H = 1.2$.

As microwaves propagate through the atmosphere to the sensor from ground surfaces, the absorption, scattering and emission occur. Atmospheric effects are taken into account by a radiative transfer (RT) formula [18]

$$T_B = AT_{B_DMRT} + T_{air}(1 - A) + AT_{air}(1 - A)(1 - e) \quad (2)$$

where A is an empirical coefficient and varies with frequencies because of the different enhancement in brightness temperatures for different frequencies. $A = 0.9225$ for 19 GHz and 0.8831 for 37 GHz. T_{B_DMRT} is brightness temperatures of snow above ground calculated by DMRT. The quantity T_{air} is the air temperature and is assumed to be a constant with $T_{air} = 250$ K, and e is the emissivity of snow above ground as calculated by DMRT.

A set of calculated brightness temperatures with typical physical parameters is plotted in Fig. 2(a)–(c). The snow temperature is 260°K and the ground temperature is 270°K. Fractional volume is 20% and grain size various from 0.02 cm to 0.1 cm in diameter. From these figures, we find that for fixed grain sizes, brightness temperatures decrease as snow depth increases. Brightness temperatures for 37 GHz saturate at snow depth around 50 cm especially for larger grains. This saturation effect is also observed by other investigators [19]. Because of the saturation effect of 37 GHz, brightness temperature differences between 19 and 37 GHz of horizontal polarization do not always have a linear relationship with snow depth. For small grain size, differences increase with snow depth. While for the larger grain size, differences may decrease as snowpack becomes thicker.

To simply the problem, only four snow parameters—snow depth, grain size, fractional volume and snow temperature—are allowed to vary while generating training data for neural network. Other parameters such as ground temperature and surface roughness, are assumed to be constants. The ground temperature used to generate training data is 270 K. The mixing factors Q and Q_g , dependent on surface roughness, are also assumed to be constants for all snow seasons. Further studies are needed to determine how sensitive brightness temperatures are to these parameters. In order to match vertical and horizontal polarization brightness temperatures simultaneously, roughness (Q) has to be correctly modeled. Since we use a constant value for all snow seasons, we may not be able to match both polarization simultaneously. Thus, different weighting factors are imposed when matching brightness temperatures. Current training dataset can apply to snow seasons with polarization differences in brightness temperatures ($T_{BV} - T_{BH}$) of about 5 to 10°K.

Linear Regression: A Special Case of DMRT Model: A linear curve based on Chang's linear regression algorithm [2] together with a family of curves generated based on our algorithm are plotted in Fig. 3. Based on the QCA-sticky DMRT model, differences of brightness temperatures show a linear (or close to linear) relationship with snow depth for smaller grain sizes and thin snow depth. Therefore, linear regression is a special case of DMRT model.

B. Snow Hydrology Model

The snow hydrology model simulates the evolution of the snowpack over time, given the meteorological and topographical information. The meteorological variables include precipitation, air temperature, humidity, wind speed, incoming short-wave radiation, and incoming longwave radiation. For precipitation input, it is important to test the applicability of the algorithm using a weather forecast model because precipitation measurements are often not available in real time. Depending on the availability, the precipitation input can be provided either by ground station measurements or from weather forecast models,

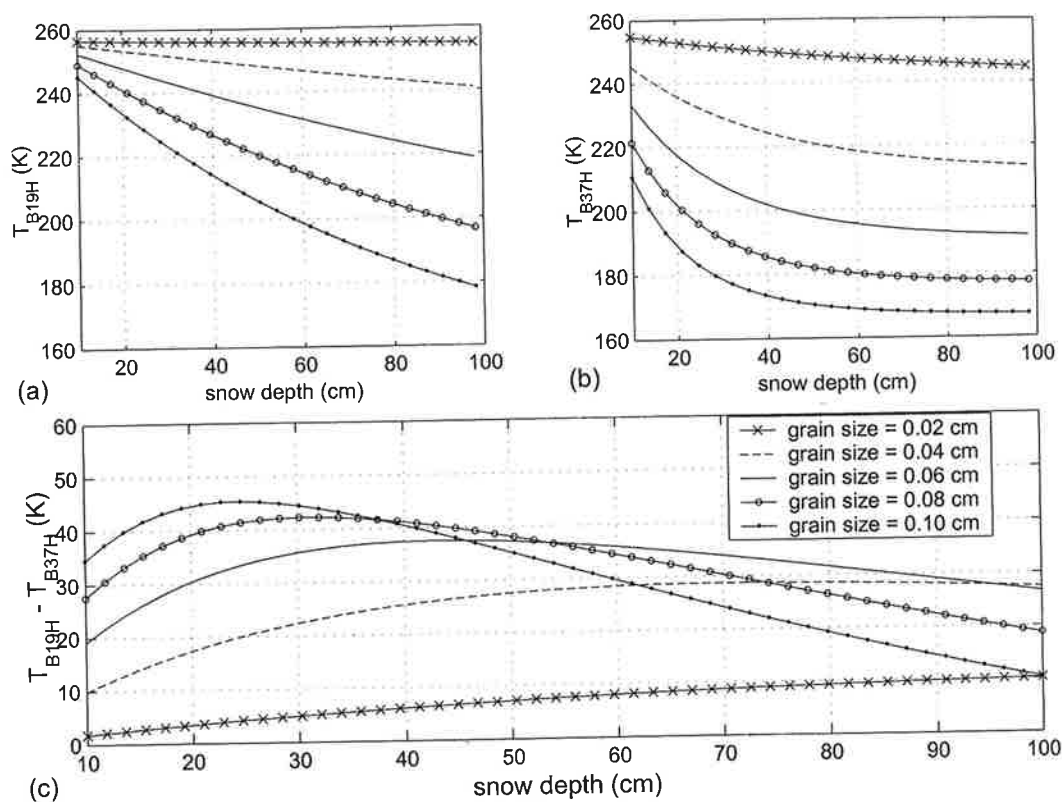


Fig. 2. Brightness temperatures of horizontal polarization as a function of the snow depth with various grain size. The snow temperature is assumed to be 260 °K, and the ground temperature is assumed to be 270 °K. The volume fraction is 20%. Atmospheric and roughness effects are included. The mixing factor Q is 0.4 and H is 1.2: (a) 19 GHz (T_{19H}), (b) 37 GHz (T_{37H}), and (c) difference of 19 and 37 GHz ($T_{19H} - T_{37H}$).

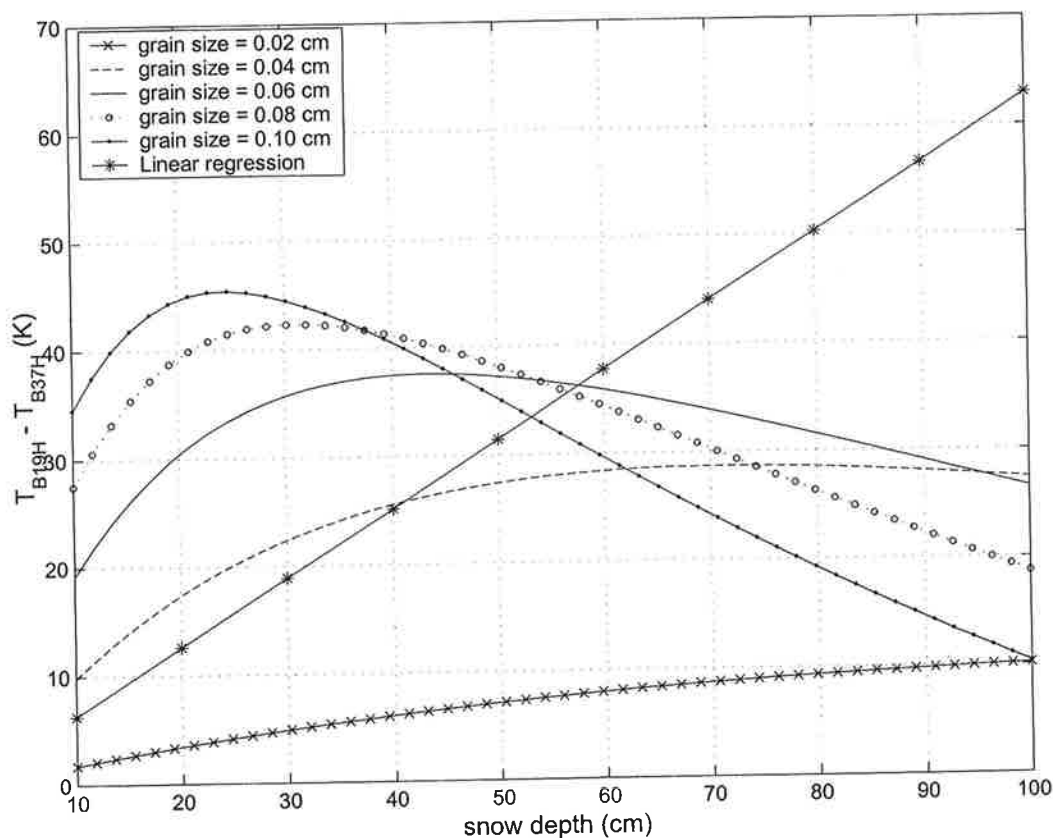


Fig. 3. Brightness temperature differences as a function of snow depth based on the linear regression algorithm and QCA-sticky DMRT model. The same parameters as in Fig. 2 are used to generate this set of curves for DMRT model.

such as the NCEP weather forecast model and that of the European Centre for Medium-Range Weather Forecasts (ECMWF). Topographic information is used to spatially distribute and lapse the meteorological data and to account for slope and aspect topographic effects on incoming solar radiation.

The snow hydrology model was originally developed as part of the distributed hydrology-soil-vegetation model (DHSVM) [20], [21]. Snow accumulation and melt are simulated using a two-layer energy-balance model that explicitly incorporates the effects of topography and vegetation cover on energy exchange at the snow surface. During melt conditions, the snowpack is assumed isothermal at 0 °C. The model accounts for net radiation, sensible and latent heat exchange, and the energy advected by rain. Precipitation below a threshold temperature is assumed to be snow, which is added to the amount of water stored in the snowpack. The model accounts for the cold content of the snowpack, which must be satisfied before melt can occur. The original snow model from DHSVM predicted snow temperature and SWE, but did not predict snow grain size and snow density. For the current application, the snow model was adapted to allow prediction of these variables as well.

The snow hydrology model simulates the mass and heat balance. The snowpack is divided into two layers, a thin surface layer and a deeper layer. Only the surface layer interacts directly with the atmosphere. Consequently, energy exchange between the atmosphere, the vegetation and the snowpack occurs to and from the surface layer. Energy exchange between the surface and the deeper layer occurs via melt water that percolates from the surface layer into the pack. In the current implementation, the snow surface layer is the minimum of the entire pack water equivalent or 0.125 m of water equivalent. The energy balance of the snow surface is given by

$$C_s W \frac{dT_s}{dt} = Q_r + Q_s + Q_e + Q_p + Q_m \quad (3)$$

where

- C_s heat capacity of ice;
- W water equivalent of the snow surface layer;
- T_s temperature of the snow surface layer;
- t time;
- Q_r net radiative flux;
- Q_s sensible heat flux;
- Q_e latent heat flux;
- Q_p energy advected by rain;
- Q_m energy lost by the snow surface layer when a portion of the layer melts or gained when liquid water in the layer refreezes.

All the components of the energy balance (except Q_p) depend on the temperature T_s of the surface layer. Each model time step is solved iteratively to find a new snow surface temperature.

The water balance of the snowpack is given by

$$\frac{dW_t}{dt} = P + C - S - O \quad (4)$$

where

- W_t total amount of water stored in the snowpack;
- P amount of precipitation including mass released from the canopy storage;

- C condensation onto the snowpack;
- S sublimation from the snowpack;
- O liquid snowpack outflow including snow melt and any liquid precipitation that cannot be stored in the snowpack.

Snow fractional volume is required as an input for the DMRT model, therefore, its initial estimate must also be provided. Snow density ρ_s and fractional volume f_v have the following relationship:

$$f_v = \frac{\rho_s}{\rho_i} \quad (5)$$

where ρ_i is the density of solid ice (910 kg/m³). Given the snow density and the SWE, the snow depth d_s can be calculated as

$$d_s = \frac{W \rho_w}{\rho_s} \quad (6)$$

where ρ_w is the density of water. We calculate snow density ρ_s in the following manner.

Snow density changes due to compaction as a result of overburden pressure were modeled in a manner similar to SNTherm [22]. However, instead of calculating this compaction for each layer individually, as is done in SNTherm, only one calculation is made for the entire snowpack as follows [10].

The average overburden pressure p_0 is given by

$$p_0 = 0.5g\rho_w W \quad (7)$$

where g is the gravitational acceleration. Given the overburden pressure, the resulting change in snow depth is calculated as

$$\Delta D_{s,t} = -\frac{p_0}{\eta} D_{s,t-1} \Delta t \quad (8)$$

where

- η viscosity of the snow (which is a function of temperature and density);
- $\Delta D_{s,t}$ change in depth at time t ;
- $D_{s,t-1}$ snow depth before the overburden pressure is applied.

The new snow depth $D_{s,t}$ is then calculated as the sum of $D_{s,t-1}$ and $\Delta D_{s,t}$. The new density ρ_s is calculated as

$$\rho_s = \frac{W}{D_{s,t}} \quad (9)$$

For the current application, the initial density of freshly fallen snow was assumed to be 80 kg/m³.

A rudimentary grain growth algorithm was implemented in the snow hydrology model. Jordan identifies two separate cases in SNTherm in [22]: dry snow layers and wet snow layers. For a dry snowpack, SNTherm parameterizes grain size growth as a function of the thermal gradient in the snowpack. Because our snow hydrology model only calculates a temperature for the surface layer, it is not possible to calculate the thermal gradient in the snowpack. Instead, we calculate an average grain size increase based on the formulation for near isothermal snowpacks in SNTherm. The grain size g_s (diameter) is calculated as

$$g_{s,t} = g_{s,t-1} + \frac{g_2}{g_{s,t-1}} m \Delta t \quad (10)$$

where g_2 is a constant ([22] suggests $4.0 \times 10^{-12} \text{ m}^2/\text{s}$), and m is a multiplier that varies linearly as a function of the wetness of the snowpack. For a dry snowpack m is equal to 0.05, while for a wet snowpack it is equal to 0.14. For the current application, the initial snow grain diameter of freshly fallen snow as assumed to be $4.0 \times 10^{-5} \text{ m}$.

C. Neural Network Inversion

For a timely inference of snow depth from observed measurement vector m , the neural network is used to speed up the parameter retrievals.

The neural network is first trained through the backpropagation (BP) algorithm by input–output combinations provided by the DMRT model. The training data contains inputs of snow parameters including snow depth, grain size, fractional volume, snow physical temperature and the four brightness temperature outputs (at 19V, 19H, 37V and 37H). The back propagation training process can be expressed by the following:

$$w_{kji} \leftarrow w_{kji} + \Delta w_{kji} = w_{kji} + \eta \cdot \delta_{k,j} \cdot y_{k-1,i} \quad (11)$$

where

- w_{kji} synaptic weight connected the j th neuron in layer k to the i th neuron in layer $(k-1)$;
- η learning rate parameter;
- $y_{k-1,i}$ output of the i th neuron in layer $(k-1)$;
- $\delta_{k,j}$ local gradient of the j th neuron in layer k , which can be obtained by backpropagating error between actual output and desired output in the top layer of the neural network.

After training, the weights of the neural network are determined. The neural network then inverts snow parameters from satellite SSM/I measurements by incorporating result of the snow hydrology model. The inversion method uses an idea similar to the BP algorithm, where error signals are back propagated to determine inputs in the manner of changing inputs so that output error decreases. The inversion process can be written as

$$\alpha_{0,i} \leftarrow \alpha_{0,i} + \eta \Delta \alpha_{0,i} = \alpha_{0,i} + \eta \varphi'_i(\alpha_{0,i}) \sum_j w_{1ji} \cdot \delta_{1,j} \quad (12)$$

where

- $\alpha_{0,i}$ i th input to the neural network;
- φ_i activation function describing the input–output functional relationship of the nonlinearity associated with the i th neuron in the input layer;
- w_{1ji} weight connecting j th neuron in first hidden layer and the i th input to the neural network;
- $\delta_{1,j}$ local gradient of the j th neuron in the first layer;
- η learning rate parameter.

IV. RESULTS AND DISCUSSION

In this section, two sets of results are presented. In the first set of results given in Section IV-A, ground precipitation measurements are used to implement the snow hydrology model. In the second set of results given in Section IV-B, the NCEP forecast model is used to provide precipitation inputs

TABLE I
NAME, LOCATION, AND ELEVATION OF THE GROUND STATIONS

| Station Number | Name | Latitude | Longitude | Elevation (m) |
|----------------|------------------|----------|-----------|---------------|
| 23226 | Vorkuta | 67°29N | 64°01E | 180 |
| 24382 | Ust'-Moma | 66°27N | 143°14E | 196 |
| 28696 | Kalacinsk | 55°02N | 74°35E | 107 |
| 28748 | Troick | 54°06N | 61°35E | 193 |
| 29789 | Verhnjaja Gutara | 54°13N | 96°58E | 984 |
| 38462 | Pskern | 41°54N | 70°22E | 1258 |
| 47005 | Samjiyon | 41°49N | 128°19E | 1386 |
| 70231 | McGrath | 62°58N | 155°37W | 103 |

for the snow hydrology model. Precipitation predicted by weather forecast models differ from real precipitation measured on the ground and thus estimated SWE from the snow hydrology model may incorporate model precipitation errors. Therefore, for the second set of results, we impose additional constraints on grain size growth and snow density evolution. The algorithm has been applied to 100 ground stations in the Northern Hemisphere. In the section, results are illustrated for selected stations. Comparisons of simulated snow depth, with and without microwave-based updating, against ground truth measurements are shown for different snow seasons. The ground station information is given in Table I.

A. Results with Station Precipitation Inputs

Results for two snow seasons at three different stations are shown. Fig. 4 shows a set of typical results for the sites in Siberia (Station 24382, Ust'-Moma). Thin to moderate snowpacks are observed in winters 1993–1994 and 1994–1995. Satellite brightness temperature measurements over this site have large differences of horizontal polarization between 19 and 37 GHz. Thus, the linear regression technique tends to overestimate snow depth. Our algorithm, on the other hand, models snow parameters besides depth and yields better estimates in snow depth. For the first snow season (1993–1994), estimates of snow depth compare favorably with ground-truth measurements in the early snow season, while snow depth is underpredicted toward the end of the season. The neural network updating amount is fairly small in the early season. For the late snow season, the updating takes place and the snow depth prediction is improved. Even though our algorithm slightly overestimates snow depth during certain periods for this season, the overall prediction of depth is quite good. For the second season (1994–1995), the snow depth is constantly underestimated. The updating again improves the predictions. Another site in former USSR (Station 29789, Verhnjaja Gutara) with thin to moderate snowpacks is shown in Fig. 5. For winter 1993–1994, the simulated snow depth agrees well with ground-truth observation, especially in the early accumulation season. The updating during mid November is in the right direction but the amount is too large. The continuing updating is able to improve the prediction and the predicted snow depth reflects ground truth measurements closely until the end of the season. For winter 1994–1995, snow depth is constantly underestimated, while the updating improves the estimates. For both seasons, the snow hydrology

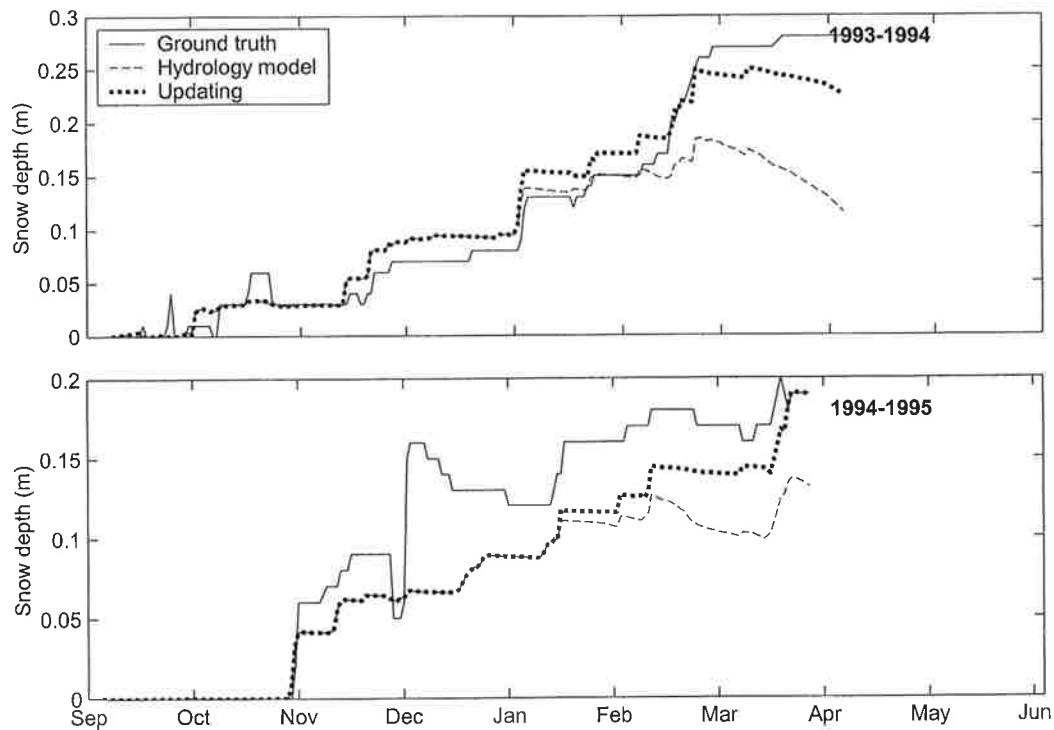


Fig. 4. Comparison of simulated snow depth (in meters) with and without microwave-based updating against ground truth measurements at Ust'-Moma (former USSR), latitude $66^{\circ}27'N$, longitude $143^{\circ}14'E$, with thin to moderate snowpacks. Solid line: ground-truth measurements. Dotted line: results with microwave-based updating. Dashed line: results from snow hydrology simulation without updating.

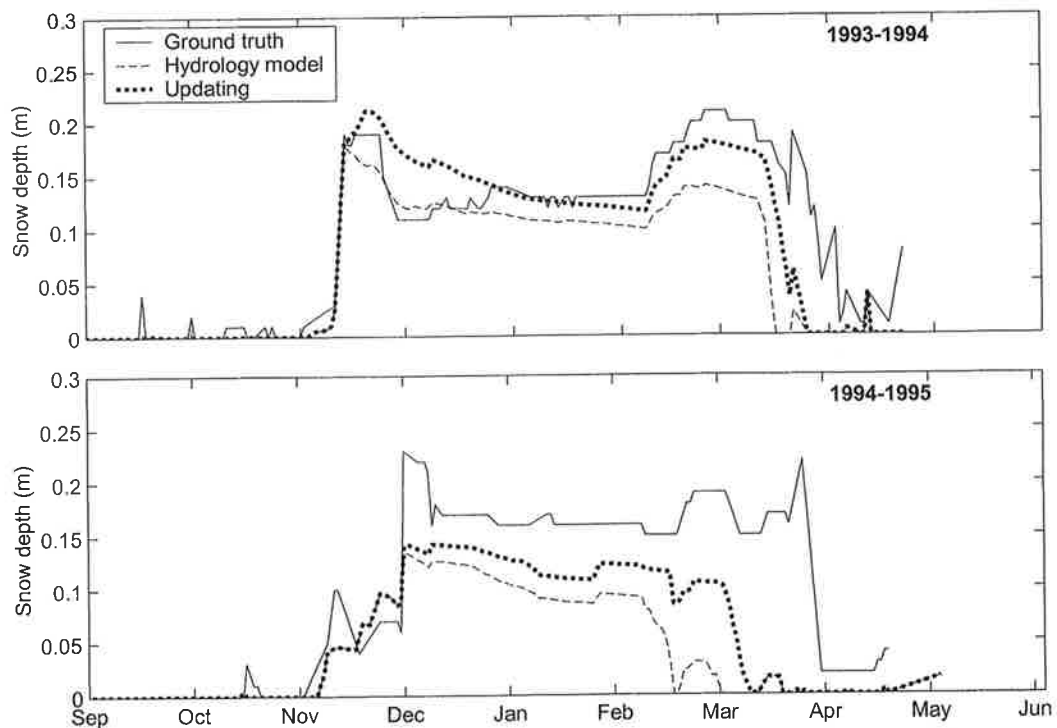


Fig. 5. Comparison of simulated SWE with and without microwave-based updating against ground truth measurements at Verhnjaja Gutara (former USSR), latitude $54^{\circ}13'N$, longitude $96^{\circ}58'E$, with thin to moderate snowpacks. Solid line: ground truth measurements. Dotted line: results with microwave-based updating. Dashed line: results from snow hydrology simulation without updating.

model predicts snowmelt much earlier than the actual occurrence. The updating does not seem to work well at the end of the seasons, possibly due to wet snowpacks. A deep snowpack case is shown in Fig. 6. This is a low elevation site in central

Alaska (Station 70231, McGrath), west of the Alaska Range and east of the Kuskowin Mountains, with long cold winters. Absolute brightness temperatures are quite low for all snow seasons, while differences between 19 and 37 GHz are small.

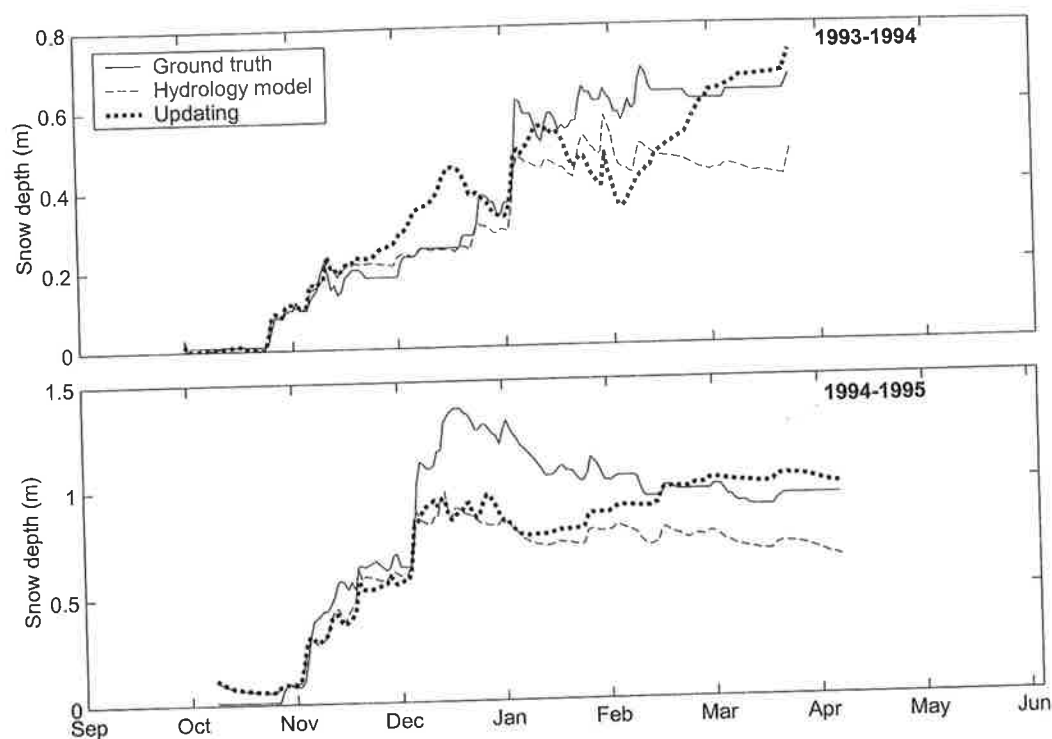


Fig. 6. Comparison of simulated SWE with and without microwave-based updating against ground truth measurements at McGrath (Alaska, USA), latitude $62^{\circ}58'N$, longitude $155^{\circ}37'W$, with deep snowpacks. Solid line: ground truth measurements. Dotted line: results with microwave-based updating. Dashed line: results from snow hydrology simulation without updating.

The linear regression technique, therefore, constantly underestimates snow depth. Simulated snow depth, however, compares favorably with ground truth measurements. The neural network updating improves the estimates in the second snow season (1994–1995). However, the updating is not always in the right direction in the first season. The updated results match well with ground truth at the end of both snow seasons.

Among the 100 sites that are simulated by our algorithm, over 50 sites have less than 10 cm of the mean absolute error of predicted snow depth. Forced by meteorological station precipitation measurements, the snow hydrology model provides fairly good estimates of snow depth (SWE). Generally, the neural network performs minor updating of the estimates since initial values are quite good already. It is shown that results of this algorithm give good predictions on snow depth of dry snowpacks with ground precipitation measurements. When the liquid water content increases in snowpacks to give wet snow toward the end of snow seasons, the performance declines.

B. Results with NCEP Reanalysis Inputs

The snow hydrology model requires precipitation inputs in order to simulate the snowpack evolution, yet real time precipitation measurements are often not available. Also precipitation measurement stations can be sparsely distributed over many parts of the world. If the algorithm is to perform in real-time, it is important to test the applicability of the algorithm using weather forecast models to provide precipitation inputs for the snow hydrology model. In this study, NCEP reanalysis project inputs are used. The predicted precipitation from the NCEP model can differ from meteorological station precipita-

tion observation. Thus, estimated snow depth from the snow hydrology model can contain substantial differences from ground truth snow depth. In such cases, the neural network updating plays a significant role in estimating snow depth. To reduce the consequence of the deficiencies in NCEP inputs, constraints based on prior knowledge are used. In this study, constraints on snow grain size growth and snow density evolution are imposed on the inversion scheme. We first classify the grain size growth into several types, using a vector quantization (VQ) technique. Snow grain size growth for each snow season at weather stations must be determined before classification. Estimates of snow temperatures from the hydrology model are assumed to be reliable. To establish constraints on grain sizes, we used ground truth snow depth measurements, snow hydrology model density and snow temperature to determine the snow grain size that gives brightness temperatures matching SSM/I brightness temperature measurements. This is done at 100 stations for three snow seasons. After obtaining the grain size growth at each station in this manner, we then use vector quantization to classify snow grain size into 32 types. During the inversion, classified grain size growth curves are used to impose constraints on the grain size growth instead of using the snow hydrology model predicted grain size. Similar methods can be used to classify snow density evolution.

Fig. 7 shows the results of a site over Siberia (Station 23226, Vorkuta). This site is located just above the Arctic Circle and has very long, cold winters, and frequently, deep snowpacks. The NCEP reanalysis underestimates precipitation, therefore, the snow hydrology model underpredicts snow depth over these three snow seasons. Neural network updating with additional constraints on grain size and density improves the estimates by

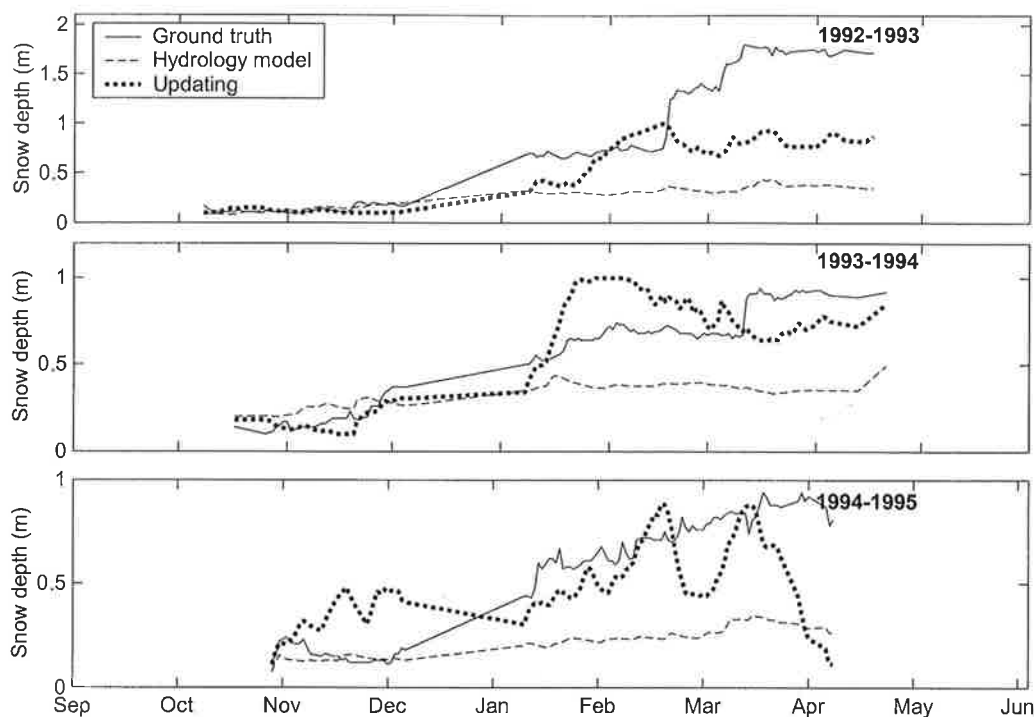


Fig. 7. Comparison of simulated SWE with and without microwave-based updating against ground truth measurements at Vorkuta (former USSR), latitude $67^{\circ}29'$ N, longitude $64^{\circ}1'$ E, with deep snowpacks. Solid line: ground truth measurements. Dotted line: results with microwave-based updating. Dashed line: results from snow hydrology simulation without updating.

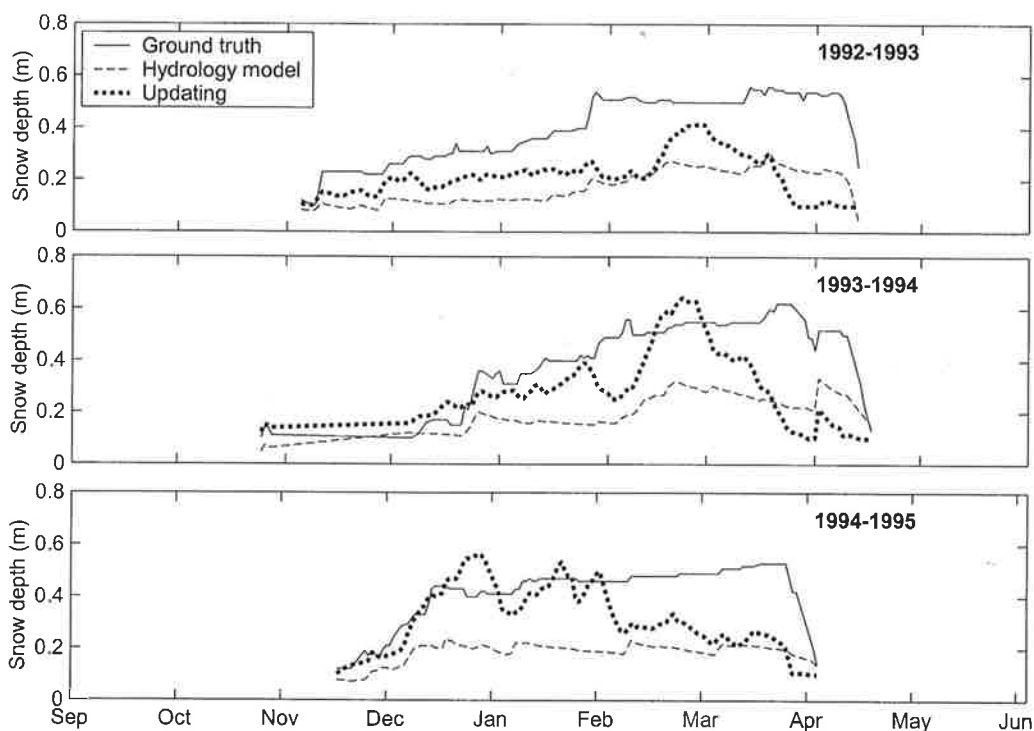


Fig. 8. Comparison of simulated SWE with and without microwave-based updating against ground-truth measurements at Kalacinsk (former USSR), latitude $55^{\circ}2'$ N, longitude $74^{\circ}35'$ E, with moderate snowpacks. Solid line: ground truth measurements. Dotted line: results with microwave-based updating. Dashed line: results from snow hydrology simulation without updating.

a fairly large amount especially for mid to late snow seasons. In the winter of 1992–1993, a maximum snow depth of about 1.7 m was observed. However, the snow hydrology model only predicts a snow depth of 0.4 m. With the updating scheme, we

are able to improve the prediction to about 0.9 m. In the winter of 1993–1994, the snow hydrology predictions match observed ground-truth snow depth quite well in the early snow season. Late in the season, however, the snow hydrology model under-

Fig. 9
longit
result

pred
dict
at th
and
diffe
drol
neur
hydr
mid
the p

F
Low
erate
snow
dati
earl
proc
dict
199
cho
ture
be e
the
the

A
(Sta
goo
Neu
not
199
the

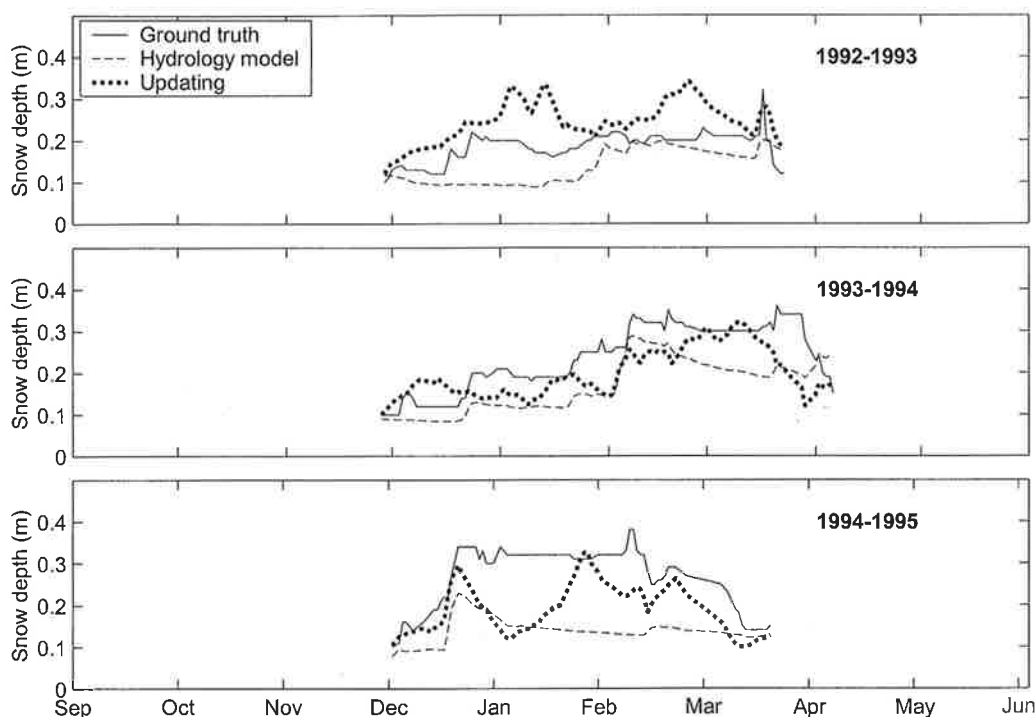


Fig. 9. Comparison of simulated SWE with and without microwave-based updating against ground truth measurements at Troick (former USSR), latitude $54^{\circ}6'N$, longitude $61^{\circ}35'E$, with thin to moderate snowpacks. Solid line: ground truth measurements. Dotted line: results with microwave-based updating. Dashed line: results from snow hydrology simulation without updating.

predicts snow depth. With neural network updating, the predicted maximum snow depth can be improved by about 0.4 m at the end of the season. The difference between the observed and predicted snow depth is 0.1 m, while without updating the difference, it is 0.4 m. In the season of 1994–1995, the snow hydrology model performs well in the early snow season while the neural network updating overestimates snow depth. The snow hydrology model, however, underpredicts snow depth in the mid-late season, while the updating scheme is able to improve the prediction.

Fig. 8 presents a site east of Omsk in the Western Siberian Lowland (Station 28696, Kalacinsk) with cold winters and moderate snowpacks. The snow hydrology model underpredicted snow depth. In the winter of 1992–1993, neural network updating can somewhat improve the snow depth estimates in the early-mid snow season. At the end of this season, the updating produced changes in the wrong direction, worsening the predicted snow depth. A similar situation occurred in the winter of 1993–1994 and 1994–1995. The neural network at some point chose a wrong update value and was not able to correct it in future timesteps. Another possibility is that air temperature may be estimated incorrectly. Simulated snow depth decreases, while the ground-truth snow depth is still increasing, suggesting that the melting event might be predicted too early in the seasons.

A site with thin to moderate snowpacks is shown in Fig. 9 (Station 28748, Troick). NCEP reanalysis gives reasonably good precipitation estimates for some of the snow seasons. Neural network updating during those snow seasons does not always improve snow depth estimates. In the winter of 1992–1993, even though the updating is in the correct direction, the updating amount is larger than that of the ground truth.

For the snow season of 1993–1994, predicted snow depth for both snow hydrology model and updating compares well with ground measurements. In the winter of 1994–1995, neural network updating is able to improve the predictions for most of the time of the season.

Fig. 10 shows the results of a high elevation site (elevation 1258 m) in the Alatua mountains northwest of Tashkent (Station 38462, Pskem). This site has moderately cold, humid winter and deep snowpacks. NCEP generally underpredicts precipitation by a large amount. The snow hydrology model underpredicts snow depth over all the seasons. Together with neural network updating, we are able to improve the estimates by some amounts. The updating amount, however, is not large enough to match observed snow depth.

Two snow seasons are modeled at Station 47005, Samjiyon (Fig. 11). This is a high elevation site (elevation 1386 m) in northern North Korea. It has cold winters and moderately deep snowpacks. NCEP reanalysis underpredicts precipitation. Therefore, the snow hydrology model predicts shallow snow depth. The neural network updating improves the predicted snow depth though is not large enough to match the observation.

The results show that even with inaccurate precipitation predictions, the neural network updating process can improve the hydrologic predictions of snow depth or SWE if additional constraints are imposed particularly on snow grain size and density during inversion.

V. CONCLUSION

This study showed that the combination of a snow hydrology model and the satellite SSM/I brightness temperature measurements improves estimates of the SWE or snow depth derived

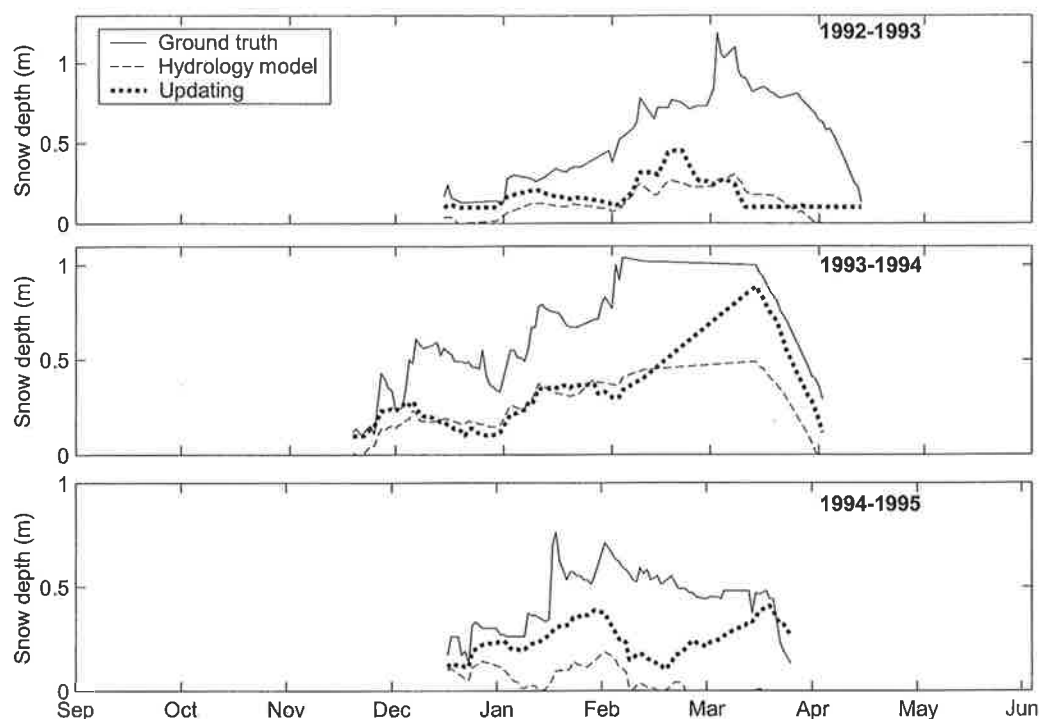


Fig. 10. Comparison of simulated SWE with and without microwave-based updating against ground truth measurements at Pskem (former USSR), latitude $41^{\circ}54'N$, longitude $70^{\circ}22'E$, with deep snowpacks. Solid line—ground truth measurements. Dotted line—results with microwave-based updating. Dashed line—results from snow hydrology simulation without updating.

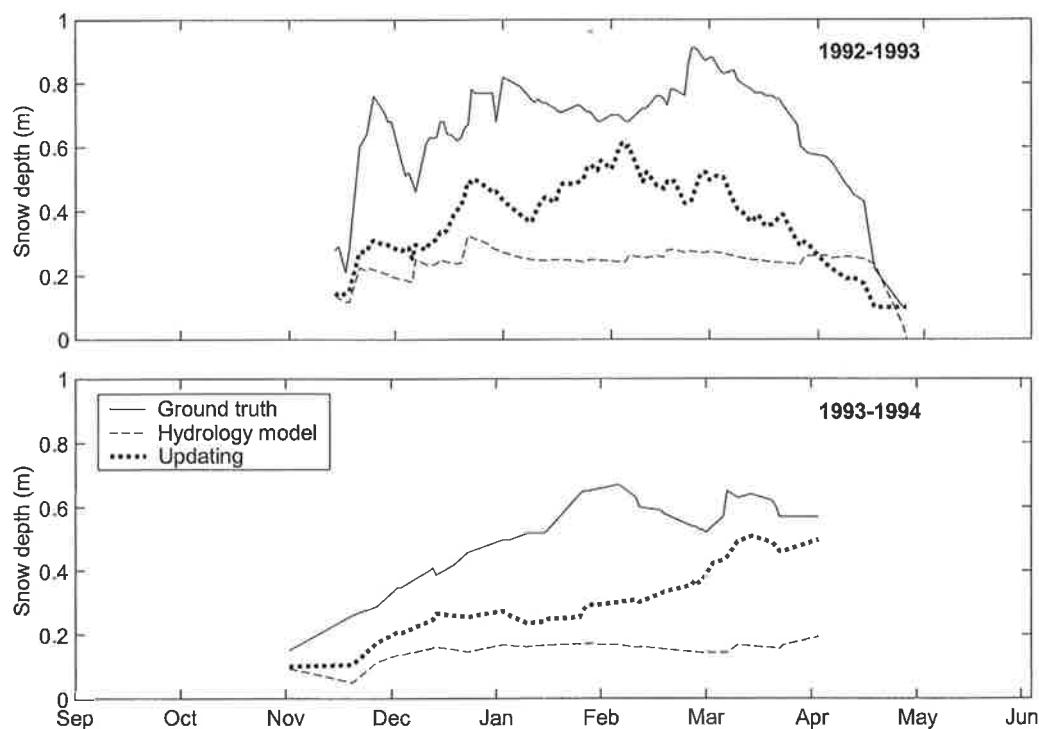


Fig. 11. Comparison of simulated SWE with and without microwave-based updating against ground truth measurements at Samjiyon (North Korea), latitude $41^{\circ}49'N$, longitude $128^{\circ}19'E$, with moderately deep snowpacks. Solid line: ground truth measurements. Dotted line: results with microwave-based updating. Dashed line: results from snow hydrology simulation without updating.

separately from each source. The physically-based snow hydrology model (a snow accumulation and ablation model) incorporates meteorological and topographical information and provides initial guesses for the neural network inversion. A DMRT

model based on QCA with the sticky particle model is used. A neural network is used to quantify the constraints and for speedy retrievals. The neural network is first trained based on the training data provided by DMRT model.

We applied the parameter retrieval algorithm to 100 stations in the northern hemisphere. Unlike linear regression techniques, which only use a subset of passive microwave remote sensing measurements, brightness temperatures of both vertical and horizontal polarization for 19 and 37 GHz are utilized. In addition to snow depth, other snow parameters are also modeled since they affect brightness temperatures.

Two sets of results are shown. For the cases which we use ground truth precipitation data, estimates of SWE from the snow hydrology model give good results. For the second case, a weather forecast model is used to provide precipitation inputs for the snow hydrology model, and the snow hydrology model performance declines. However, with additional constraints based on prior knowledge of snow grain size and density, the retrieval algorithm is able to improve the estimates of snow parameters.

REFERENCES

- [1] A. T. C. Chang, J. L. Foster, D. K. Hall, A. Rango, and B. K. Hartline, "Snow water equivalent estimation by microwave radiometry," *Cold Regions Sci. Technol.*, vol. 5, no. 3, pp. 259–267, 1982.
- [2] A. T. C. Chang, J. L. Foster, and D. K. Hall, "Nimbus-7 SMMR derived global snow cover parameters," *Ann. Glaciol.*, vol. 9, pp. 39–44, 1987.
- [3] B. E. Goodison, "Determination of areal snow water equivalent on the Canadian prairies using passive microwave satellite data," in *Proc. IEEE Int. Geoscience and Remote Sensing Symp.* '89, vol. 3, Vancouver, BC, Canada, 1989, pp. 243–246.
- [4] A. Rango, J. Martinec, A. T. C. Chang, J. L. Foster, and V. F. van Katwijk, "Average areal water equivalent of snow in a mountain basin using microwave and visible satellite data," *IEEE Trans. Geosci. Remote Sensing*, vol. 27, pp. 740–745, Nov. 1989.
- [5] A. T. C. Chang, J. L. Foster, and A. Rango, "Utilization of surface cover composition to improve the microwave determination of snow water equivalent in a mountain basin," *Int. J. Remote Sensing*, vol. 12, pp. 2311–2319, Nov. 1991.
- [6] M. T. Hallikainen and P. A. Jolma, "Comparison of algorithms for retrieval of snow water equivalent from Nimbus-7 SMMR data in Finland," *IEEE Trans. Geosci. Remote Sensing*, vol. 30, pp. 124–131, Jan. 1992.
- [7] J. R. Wang, A. T. C. Chang, and A. K. Sharma, "On the estimation of snow depth from microwave radiometric measurements," *IEEE Trans. Geosci. Remote Sensing*, vol. 30, pp. 785–792, July 1992.
- [8] R. L. Armstrong and M. J. Brodzik, "An Earth-gridded SSM/I data set for cryospheric studies and global change monitoring," *Adv. Space Res.*, vol. 16, no. 10, pp. 155–163, 1995.
- [9] J. L. Foster, A. T. C. Chang, and D. K. Hall, "Comparison of snow mass estimates from prototype passive microwave snow algorithm, a revised algorithm and a snow depth climatology," *Remote Sens. Environ.*, vol. 62, no. 2, pp. 132–142, 1997.
- [10] L. Wilson, L. Tsang, J.-N. Hwang, and C.-T. Chen, "Mapping snow water equivalent in mountainous areas by combining a spatially distributed snow hydrology model with passive microwave remote sensing data," *IEEE Trans. Geosci. Remote Sensing*, vol. 37, pp. 690–704, Mar. 1999.
- [11] T. Koike, E. Togashi, and H. Fujii, "Validation and application of a snow algorithm in the Eurasian continent," in *Proc. IEEE Int. Geoscience and Remote Sensing Symp.* '00, Honolulu, HI, 2000, pp. 1558–1560.
- [12] A. E. Walker and B. E. Goodison, "Challenges in determining snow water equivalent over Canada using microwave radiometry," in *Proc. IEEE Int. Geoscience and Remote Sensing Symp.* '00, Honolulu, HI, 2000, pp. 1551–1554.
- [13] A. W. England, "Thermal microwave emission from a halfspace containing scatterers," *Radio Sci.*, vol. 9, no. 4, pp. 447–454, 1974.
- [14] —, "Thermal microwave emission from a scattering layer," *J. Geophys. Res.*, vol. 80, no. 32, pp. 4484–4496, 1975.
- [15] L. Tsang, J. A. Kong, and R. Shin, *Theory of Microwave Remote Sensing*. New York: Wiley, 1985.
- [16] L. Tsang, C.-T. Chen, A. T. C. Chang, J. Guo, and K.-H. Ding, "Dense media radiative transfer theory based on quasicrystalline approximation with applications to passive microwave remote sensing of snow," *Radio Sci.*, vol. 35, no. 3, pp. 731–749, 2000.
- [17] J. R. Wang, P. E. O'Neill, T. J. Jackson, and E. T. Engman, "Multifrequency measurements of the effects of soil moisture, soil texture and surface roughness," *IEEE Trans. Geosci. Remote Sensing*, vol. 21, pp. 44–51, Jan. 1983.
- [18] S. Yueh, W. J. Wilson, S. J. Dinardo, and F. K. Li, "Polarimetric microwave brightness signatures of ocean wind directions," *IEEE Trans. Geosci. Remote Sensing*, vol. 37, pp. 949–959, Mar. 1999.
- [19] S. Rosenfeld and N. C. Grody, "Metamorphic signature of snow revealed in SSM/I measurements," *IEEE Trans. Geosci. Remote Sensing*, vol. 38, pp. 53–63, Jan. 2000.
- [20] M. S. Wigmosta, L. W. Vail, and D. P. Lettenmaier, "A distributed hydrology-vegetation model for complex terrain," *Water Resources Res.*, vol. 30, no. 6, pp. 1665–1679, 1994.
- [21] P. Storck, D. P. Lettenmaier, B. A. Connelly, and T. W. Cundy, "Implications of forest practices on downstream flooding, Phase II final report," Univ. Washington, Seattle, WA, July 1995.
- [22] R. Jordan, "A one-dimensional temperature model for a snow cover—Technical documentation from SNThERM," U.S. Army Corps Eng., Cold Region Res. Eng. Lab., Hanover, NH, 1991.

Chi-Te Chen (S'98) received the B.S. degree in electrical engineering from the National Taiwan University, Taipei, Taiwan, R.O.C., in 1994, and the M.S. degree from the University of Washington, Seattle, in 1996, where she is currently pursuing the Ph.D. degree.

Her research interests include theoretical and numerical studies of electromagnetic wave scattering and propagation in random media and remote sensing.

Bart Nijssen, photograph and biography not available at the time of publication.

Jianjun Guo was born in Tianmen, Hubei Province, China. He received the B.S. and M.S. degrees in electrical engineering from Wuhan University, Wuhan, China, and the University of Science and Technology of China in 1995 and 1998, respectively. He is currently pursuing the Ph.D. degree in the Department of Electrical Engineering, University of Washington, Seattle.



Leung Tsang (S'73–M'75–SM'85–F'90) was born in Hong Kong. He received the S.B., S.M., E.E., and Ph.D. degrees from the Massachusetts Institute of Technology, Cambridge.

He is currently a Professor of electrical engineering with the University of Washington, Seattle. He is co-author of the book *Theory of Microwave Remote Sensing* (New York: Wiley, 1985). His current research interests include wave propagation in random media and rough surfaces, remote sensing, optoelectronics, and computational

electromagnetics.

Dr. Tsang was Editor-in-Chief of IEEE TRANSACTIONS ON GEOSCIENCE AND REMOTE SENSING from 1996 to 2001. He was the Technical Program Chairman of the 1994 IEEE Antennas and Propagation International Symposium and URSI Radio Science Meeting, the Technical Program Chairman of the 1995 Progress in Electromagnetics Research Symposium, and the General Chairman of the 1998 IEEE International Geoscience and Remote Sensing Symposium. He is a Fellow of the Optical Society of America and the recipient of the Outstanding Service Award of the IEEE Geoscience and Remote Sensing Society for 2000. He is also the Recipient of the IEEE Third Millennium Medal.

Andrew W. Wood received the M.S.E. degree in water resources planning and management from the Department of Civil and Environmental Engineering, University of Washington, Seattle, in 1995.

He spent two years as a Visiting Fellow for the U.S. Army Corps of Engineers Institute for Water Resources before returning to the University of Washington to study hydrologic forecasting for water resources management, in pursuit of a doctorate in the same department.

Jenq-Neng Hwang (M'88-SM'96-F'01) is currently an Associate Professor with the Department of Electrical Engineering, University of Washington, Seattle.



Dennis Lettenmaier received the B.S. and Ph.D. degrees from the University of Washington, Seattle, in 1971 and 1975, respectively, and the M.S. degree from the George Washington University, Washington, DC, in 1973.

He is a surface water Hydrologist, who over the last ten years has specialized in modeling land surface hydrologic processes at continental to global scales. His particular interests include prediction of the effects of climate variability and change on surface hydrologic processes, including snow accumulation and ablation, and application of remote sensing to hydrologic prediction.